Journal of Geoscience and Environment Protection, 2026, 14(3), 288-317
https://www.scirp.org/journal/gep
ISSN Online: 2327-4344
ISSN Print: 2327-4336

Groundwater Quality Assessment in a Semi-Arid Area Western Central Senegal Using Water Quality Index (WQI) and Multivariate Statistical Analysis

Mathias Diédhiou[1*], Seyni Ndoye[2], Elie Joseph Insa Diédhiou[1], Serigne Faye[1], Philippe Le Coustumer[3], Arnaud Gauthier[4]

[1]Geology Department, Faculty of Science and Technology, Cheikh Anta Diop University, Dakar, Senegal
[2]Water-Energy-Environment-Industrial Processes Laboratory, Department of Civil Engineering, Polytechnic School, Cheikh Anta Diop University, Dakar, Senegal
[3]Bordeaux Imaging Center, University of Bordeaux, Bordeaux, France
[4]Laboratory of Civil Engineering and Geo-Environment (LGCgE, ULR 4515), JUNIA, IMT Nord Europe, University of Lille, University of Artois, Lille, France
Email: *mathias.diedhiou@ucad.edu.sn

How to cite this paper: Diédhiou, M., Ndoye, S., Diédhiou, E. J. I., Faye, S., Le Coustumer, P., & Gauthier, A. (2026). Groundwater Quality Assessment in a Semi-Arid Area Western Central Senegal Using Water Quality Index (WQI) and Multivariate Statistical Analysis. *Journal of Geoscience and Environment Protection, 14,* 288-317.
https://doi.org/10.4236/gep.2026.143013

Received: January 28, 2026
Accepted: March 24, 2026
Published: March 27, 2026

Copyright © 2026 by author(s) and Scientific Research Publishing Inc.
This work is licensed under the Creative Commons Attribution International License (CC BY 4.0).
http://creativecommons.org/licenses/by/4.0/
Open Access

Abstract

Water quality is a very significant parameter that determines its suitability for various uses. In this study, 42 groundwater samples were collected, 39 of which were ultimately used after calculating the ion balance error, from wells and boreholes during a sampling campaign conducted from May 30 to June 1, 2023, to assess quality and identify the main factors controlling groundwater chemistry. The results show that the pH ranges from 6.89 to 8.2, indicating that the groundwater is neutral to alkaline in nature. The order of abundance of ions in groundwater is defined as follows: $HCO_3^- > Cl^- > SO_4^{2-} > NO_3^-$ for anions and $Na^+ > Ca^{2+} > Mg^{2+} > K^+$ for cations, indicating that (HCO_3^-) and (Na^+) are respectively the most abundant anion and cation in groundwater. The piper diagram shows four water types: Ca-HCO_3 water type, Na-Cl water type, mixte-Ca-Mg-Cl water type, and Ca-Cl water type, of which Ca-HCO_3 is the dominant water type. Gibbs diagrams, binary diagrams, and chloro-alkaline index values indicate that water-rock interaction, evaporation, and ion exchange are the main processes controlling groundwater mineralization. Principal Component Analysis (PCA) identified two principal components accounting for 80.54% of the total variance. The first component indicates that water quality is controlled by natural processes such as water/rock interaction and evaporation, but also by anthropogenic pollution. The second component is associated with fluoride-rich alkaline waters, suggesting the in-

fluence of fluoride-bearing minerals dissolution. Furthermore, Hierarchical Cluster Analysis (HCA) classified the waters into two groups: highly mineralized waters with a mean TDS value of 2642.5 mg/L and moderately mineralized alkaline waters with a mean TDS value of 666.7 mg/L. The water quality index (WQI) of the study area ranged from 4 to 414 and shows that the majority of water (64%) is unfit for human consumption.

Keywords

Principal Component Analysis (PCA), Hierarchical Cluster Analysis (HCA), Groundwater Quality, Water Quality Index (WQI), Groundwater Mineralization

1. Introduction

Groundwater is an important natural resource that is essential to the survival and development of all living organisms. It is one of the main water resources widely used to meet the multiple needs of humans. Groundwater is used for various purposes such as human consumption, agriculture, livestock farming, food preparation, recreation, sanitation, hygiene, medicine, and industry (Tongesayi & Tongesayi, 2017). Numerous studies have shown that 65% of groundwater is used for domestic purposes, 20% for irrigation, and 15% by industry (Adimalla & Venkatayogi, 2018; Salehi et al., 2018). However, the availability of good-quality water is a major constraint in many parts of the world, particularly in densely populated and highly industrialized areas, but also in arid and semi-arid areas, where there is often a gradual decline in groundwater quality due to various human activities. In such semi-arid and arid areas, high population growth combined with agricultural activities involving excessive use of fertilizers, domestic and industrial wastewater discharges, and poor sanitation generally leads to groundwater pollution (Adimalla & Venkatayogi, 2018; Li et al., 2016). Furthermore, the multiple and intense pressures on groundwater can affect it quantitatively due to overexploitation to meet drinking water demand, leading to a drop in water table levels, but also qualitatively due to anthropogenic pollution, climate variability, and water-rock interactions (Singhal et al., 2020). Therefore, it is essential to assess groundwater quality and deepen our understanding of the processes and factors that control its chemistry in order to ensure effective and sustainable management of groundwater resources. As a result, over the past few decades, several studies have been conducted in different parts of the world to assess water quality and determine its suitability for various uses (Ani et al., 2024; Sajil Kumar et al., 2013; Salem et al., 2023; Xu & Shao, 2010). In fact, the chemical composition of water is an important parameter that determines its suitability for a specific use. Variations in the chemical composition of groundwater may result from various factors, such as water-rock interaction, ion exchange, mineral dissolution, evaporation, residence time of water

in the aquifer, domestic wastewater, irrigation runoff, and anthropogenic activities (Marghade et al., 2019). Several methodological approaches have been used in different geological environments to determine the main factors controlling groundwater chemistry (Kura et al., 2013; Ma et al., 2014; Nandimandalam, 2012). In central-western Senegal, particularly in the departments of Mbour and Fatick, which are characterized by a lack of perennial rivers, groundwater plays an important role in the socioeconomic development of the population. It is used extensively to meet the various water needs of the population due to the scarcity of surface water and strong population growth associated with the development of income-generating human activities such as tourism, agriculture, industry, and livestock farming, which can lead to a decline in groundwater levels and, especially, a decline in its chemical quality. Previous hydrogeological studies have mainly focused on the regional functioning of the Paleocene and Maastrichtian aquifers and on the occurrence of high fluoride and, to a lesser extent, nitrate concentrations (Travi & Le Coustour, 1982; Tine et al., 2011; Diédhiou et al., 2024). However, there is still a need for an integrated assessment that combines hydrogeochemical tools, multivariate statistics, and water quality indices to better distinguish natural processes from anthropogenic pressures and to map groundwater suitability at the local scale. Therefore, the present study aims to: 1) characterize the hydrogeochemical composition and facies of groundwater in the Mbour-Fatick area, 2) identify the main natural and human-related mechanisms controlling groundwater mineralization using multivariate statistical analysis, and 3) assess and map groundwater quality for drinking purposes based on the water quality index.

2. Study Area

2.1. Location of the Study Area

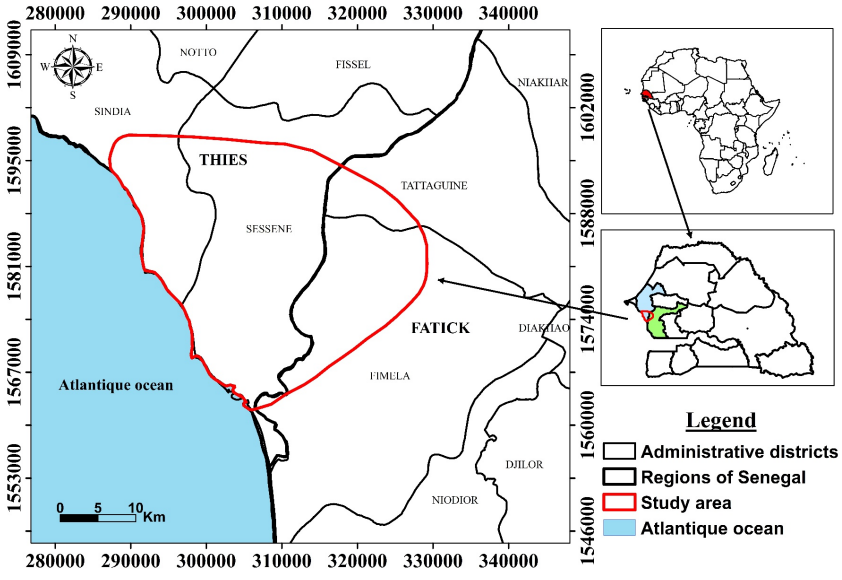

Figure 1. Location of the study area.

The study area is located in central western Senegal, in the departments of Mbour and Fatick. It encompasses part of the districts of Sindia, Sessene, Tattaguine, and Fimela, covering an area of approximately 986 km^2. It is located between longitudes 17˚02'12.6"W and 16˚35'06.7"W and latitudes 14˚27'11.3"N and 14˚35'13.9"N. It is bordered to the west by the Atlantic Ocean, to the north by the districts of Fissel and Notto, to the east by Niakhar and Diakhao, and to the south by Niodior (**Figure 1**).

2.2. Geology and Hydrogeology

The geology of the study area is part of the Senegal-Mauritania sedimentary basin, which is well known through numerous oil and water drilling investigations. These investigations have led to lithostratigraphic reconstruction and the identification of deposit environments. The study area is characterized by the presence of Quaternary and Continental Terminal geological formations consisting of detrital soils (laterite, sand, and clay) with a predominance of clay and sand. In the study area, the Eocene is heavily eroded and is represented only by its lower terms, where it consists of the following levels:

- A layer consisting of clayey limestone, marl, and clay, often enriched with phosphate or silica, which lies directly on top of the Paleocene formations (Sarr, 1982);
- A clayey or marly layer with some very frequent limestone intercalations in the upper part;
- A layer consisting of alternating limestone and marly limestone, found mainly in the Ngazobil area (Travi, 1993). The Lower and Middle Eocene are characterized by the presence of phosphate levels (Travi & Le Coustour, 1982). However, the base of the Lower Eocene consists of gray marl and clay with intercalations of flint (Saint-Marc & Sarr, 1984).

The Paleocene, in the study area, has some very distinctive features. It outcrops at Mbour and consists of limestone, clayey limestone, and marl, which are frequently enriched with flint, glauconite, and phosphate (Saint-Marc & Sarr, 1984) and sinks towards the east and southeast, where it is covered by Eocene, Continental Terminal, and Quaternary formations. It is characterized by homogeneous facies of limestone and marly limestone, often with shell deposits (Monciardini, 1966). These characteristics are indicative of shallow oceanic deposition with benthic microfauna dominated by ostracods (Diop et al., 1982). The base of the Paleocene consists of hard limestone and gray marly limestone that may be sandy (Sarr, 1999). In contrast, the Middle and Upper Paleocene are consistently formed of numerous sandy limestone levels of varying fineness and rich in shell debris (Sarr, 1982). Phosphate deposits mark the upper limits of the Paleocene limestones in the Thiadiaye and Fatick areas (Monciardini, 1966).

The Paleocene-Eocene boundary is marked by the sudden disappearance of microfauna and macrofauna and the appearance of facies that are very poor in fossils and more distinctly marine (Sarr, 1982). The transition from Paleocene

limestones to Lower Eocene marls is often marked by the deposition of a marl-clay layer containing flint, particularly in the northeastern part of the local area (Pitaud, 1980).

➢ In the hydrogeology context, two aquifer systems are found in the study area: a shallow aquifer system consisting of the Miocene-Pliocene, Quaternary, and Upper Ypresian aquifers, which are mainly tapped by traditional wells to meet the domestic and agricultural water needs of the population. The Upper Ypresian aquifer is formed of marly limestone, while the Miocene-Pliocene and Quaternary aquifers are formed of clayey sand. The Eocene limestone aquifer is distinct from or associated with the Miocene-Quaternary aquifer.

➢ A deep aquifer system, mainly tapped by modern boreholes and wells, and consisting of the deep aquifer of the Paleocene and Maastrichtian. Due to falling water levels or salinization observed in some areas of the shallow aquifers, the Paleocene aquifer is currently the most tapped. The latter is relatively thin and lies on Maastrichtian sandstone-clay sediments. It consists of limestone, clayey limestone, and marl with flint, glauconite, and phosphate (Saint-Marc & Sarr, 1984). Following a change in facies, its base, mainly composed of marl, consists of shell limestone in the west and marl in the northwest, east, and south (Tine et al., 2011). It has the following hydraulic characteristics: transmissivity varies from 5×10^{-5} m^2/s in Joal to 10^{-2} m^2/s in Louli Mbafaye (Sarr, 2003), while storage coefficients range from 1×10^{-4} to 7×10^{-2}. Hydraulic conductivity values range from 6.6×10^{-6} to 2.0×10^{-2} m/s. In the Miocene-Pliocene-Quaternary aquifer, the average values for hydraulic conductivity and effective porosity are approximately 1.5×10^{-4} m/s and 20%, respectively.

3. Materials and Methods

3.1. Groundwater Sampling and Chemical Analysis

A sampling campaign was carried out from May 30 to June 1, 2023, during which 42 samples were collected from various sampling points, including 15 boreholes and 27 wells. These sampling points were carefully selected to ensure coverage of the entire study area (**Figure 2**). The samples collected at each sampling point were filtered using a 0.45 µm pore membrane to remove suspended solids, then divided between two labeled polyethylene bottles that had been washed two or three times with the water to be collected in order to avoid contamination. Samples intended for cation analysis were acidified to lower the pH of the water below 2 by adding a 0.05 N hydrochloric acid solution in order to diminish the bacterial activities, while those intended for anion analysis were not acidified. After sampling, the collected samples were stored in coolers and then transported to the laboratory for chemical analysis. Electrical conductivity, pH, and temperature were measured in the field using a WTW multi 350i portable multi-parameter device. Chemical analyses of the collected samples were performed at the Geo-Environment Laboratory of the University of Lille in France. Anions were analyzed using

Dionex-100 ion chromatography, while cations and some metals were determined using inductively coupled plasma atomic emission spectrometry (ICP-AES). Carbonates and bicarbonates were analyzed by titrimetry using a 0.05 N sulfuric acid solution. The reliability of the chemical analyses was checked by calculating the ion balance error for each water sample using equation 1. The results indicate that three samples have ion balance error values above the acceptable limit of ±10% (Xiao et al., 2014; Yu et al., 2023) and therefore, 39 out of 42 samples were ultimately considered in the data processing.

$$IBE = \frac{\sum Cations - \sum Anions}{\sum Cations + \sum Anions} \times 100 \quad (1)$$

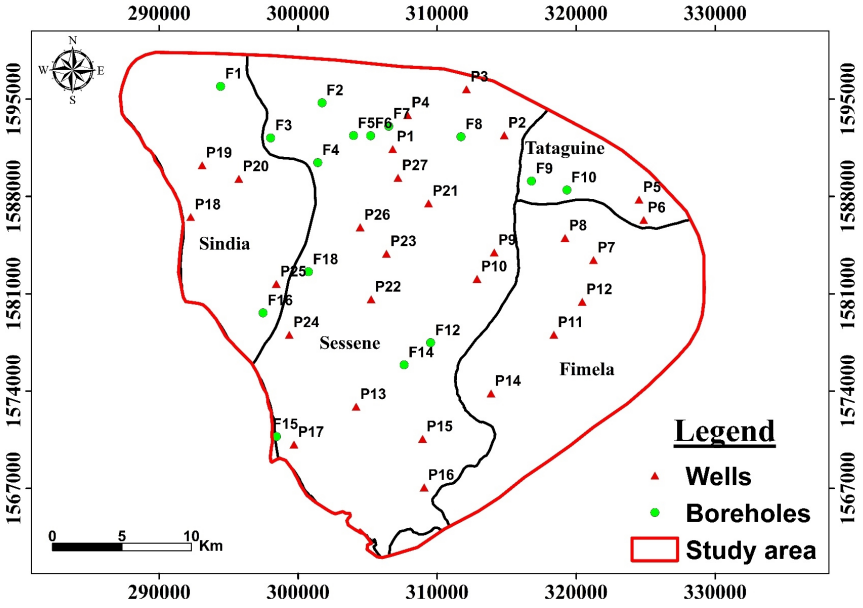

Figure 2. Sampling points in the study area.

3.2. Multivariate Statistical Analysis

Multivariate statistical analysis is a method that allows a large dataset to be reduced and organized, with minimal loss of critical information, into groups with similar characteristics (Gulgundi & Shetty, 2018; Sheikhi et al., 2021; Subba Rao, 2017). It is also used to determine similarities between water samples and water parameters (Chaudhry et al., 2019; Mohammed et al., 2022). In this study, 12 chemical parameters of water, pH, CE, HCO_3^-, Cl^-, SO_4^{2-}, F^-, NO_3^-, Ca^{2+}, Mg^{2+}, Na^+, K^+, and TDS were used to perform Principal Component Analysis (PCA), Ascending Hierarchical Analysis (AHA), and a correlation matrix. However, the data were first standardized using Equation (2) to put them on the same uniform scale (Omo-Irabor et al., 2008) in order to facilitate their interpretation and comparison.

$$Z_i = \frac{X_i - X_m}{\sigma_i} \quad (2)$$

where Z_i is a standardized variable, X_i is the raw variable, X_m is the mean of the variable, σ_i is the standard deviation.

3.2.1. Correlation Matrix

The correlation matrix is an effective statistical tool commonly used in data analysis to highlight relationships between different parameters. Pearson's correlation analysis is widely used to assess and determine the strength of a linear relationship between two variables (Selvakumar et al., 2017). A correlation is considered perfect when the correlation coefficient (r) between two variables is equal to +1 or −1 (Mohammed et al., 2022). According to Jenn et al. (2007), the strength of the correlation between variables can be divided into three levels: very high (if $0.8 \leq r \leq 1$), high (if $0.6 \leq r < 0.8$), and low (if $r < 0.6$). The correlation matrix is determined according to Equation (3) (Wang et al., 2023):

$$r = \frac{1}{n-1}\sum_{i=1}^{n}\left(\frac{x_i - \overline{x}}{\sigma_x}\right)\left(\frac{y_i - \overline{y}}{\sigma_y}\right) \tag{3}$$

where r is the correlation coefficient, n is the number of variables in the sample, x_i and y_i are the two variables to be analyzed, $\overline{x}$ and $\overline{y}$ are the mean values of x and y, σ_x and σ_y are the standard deviations of x and y.

3.2.2. Principal Component Analysis (PCA)

Multivariate statistical analysis is a technique commonly used in numerous hydrochemical studies to reduce data dimensionality (Jiang et al., 2023; Jung et al., 2021) and is essential for obtaining data on the relationships between hydrochemical variables (Salem et al., 2023). This method involves transforming the initial variables into a new coordinate system called principal components. In principal component analysis, the variable with the greatest variation is designated as the first principal component (Wang et al., 2023). The second variable with the next highest variance is identified as the second principal component, and this pattern continues successively. Taking into account the loading values, we observe a categorization into three distinct levels: strong (>0.7), moderate (0.7 - 0.5), and weak (0.5 - 0.3) (Bodrud-Doza et al., 2016; Dhakate et al., 2023). This classification shows the influence of each variable on the different principal components. Principal components with an eigenvalue greater than or equal to one (1) are considered significant and are therefore retained (Islam et al., 2017; Shuaibu et al., 2025).

3.2.3. Hierarchical Cluster Analysis (HCA)

Hierarchical cluster analysis is also a multivariate statistical method that allows variables or water samples to be classified into groups called clusters based on their similarity and dissimilarity to other groups (Kura et al., 2013; Liu et al., 2019). It is the main method for identifying relatively homogeneous clusters based on measured data (Chen et al., 2019). It is the most commonly used clustering method, which identifies the initial relationship between any sample and all data relating to water samples (Liu et al., 2019). In this study, Euclidean distance was used as

the measurement distance, allowing the proximity between different samples to be assessed. Furthermore, Ward's method was adopted to form more or less homogeneous clusters and link them together. This method evaluates the distance between clusters while minimizing the sum of the squares of the distances between two clusters formed at each stage of the classification (Fabbrocino et al., 2019). Previous studies (Güler et al., 2002; Yang et al., 2020) have shown that the use of hierarchical cluster analysis, combining Euclidean distance as a distance measure and Ward's method as a linkage rule, leads to the formation of more distinctive groups or clusters. The samples with the greatest similarity are first grouped together, and so on. This process results in the construction of a dendrogram, which is a hierarchical visual representation of the similarity relationships between the data. The number of clusters is determined based on the phenon line (Fabbrocino et al., 2019; Meng et al., 2024), and changing the location of this line on the dendrogram affects the number of clusters resulting from the classification. The Euclidean distance can be computed using Equation (4) (Liu et al., 2019):

$$D_{ik} = \sqrt{\sum_{j=1}^{m} \left(v_{ij} - v_{kj}\right)^2} \tag{4}$$

where i and k are two different water samples, j is the mode of the variables, and v is the value of the variables. The smaller the Euclidean distance D, the more similar the water samples are. The value D quantitatively indicates the degree of similarity between the water samples.

3.3. Water Quality Index (WQI)

Water quality index (WQI) is an important parameter generally computed to assess the overall water quality in a given area based on several water quality parameters. It is widely used as a tool for assessing and comparing the suitability of water for different uses, such as consumption (Xiao et al., 2014; Alfaleh et al., 2023), irrigation, and the state of aquatic ecosystems (Alfaleh et al., 2023). It considers several chemical parameters and assigns them a weight (Seifi et al., 2020). In the present study, the water quality index was computed using eleven (11) parameters: pH, HCO_3^-, Cl^-, SO_4^{2-}, F^-, NO_3^-, Ca^{2+}, Mg^{2+}, Na^+, K^+, and TDS. The calculation of the WQI involved the following steps (Bindu et al., 2023; Patel et al., 2023):

✓ The first step involves calculating the unit weight (Wn) of each water quality parameter. This step quantifies the effect of each parameter on overall water quality. The unit weight is computed using Equation (5).

$$w_n = k / S_n \tag{5}$$

where S_n is the permissible standard value according to WHO (2017; 2022), for a water quality parameter (**Table 1**). K is the proportionality constant derived from Equation (6).

$$k = \frac{1}{\sum\left(1/S_n\right)} \tag{6}$$

Table 1. Relative weight of chemical parameters.

Chemical Parameters	Units	Guideline Values (WHO, 2017; 2022)	k	W_n
pH	(-)	6.5 - 8.5	1.0673	0.081
TDS	mg/L	1000	1.0673	0.135
Ca^{2+}	mg/L	75	1.0673	0.081
Mg^{2+}	mg/L	50	1.0673	0.081
Na^{+}	mg/L	200	1.0673	0.054
K^{+}	mg/L	12	1.0673	0.054
HCO_3^-	mg/L	500	1.0673	0.027
SO_4^{2-}	mg/L	250	1.0673	0.108
Cl^-	mg/L	250	1.0673	0.108
NO_3^-	mg/L	50	1.0673	0.135
F^-	mg/L	1.5	1.0673	0.135
				$\sum W_n = 1$

✓ The second step defines the specific quality index for each quality parameter. These indices reflect the relative concentration and individual impact of the different parameters. The specific quality index (q_n) is computed using Equation (7).

$$q_n = \frac{(V_n - V_{id})}{(S_n - V_{id})} \times 100 \tag{7}$$

where V_n is the observed value of each parameter in each sample, S_n is the acceptable limit for each variable, and V_{id} is the ideal value of the i^{th} parameter in pure water. The ideal value for all parameters is 0, except for pH, which has an ideal value of 7 (Patel et al., 2023).

✓ The third step involves calculating the Water Quality Index (WQI) using Equation (8).

$$IQE = \frac{\sum q_n w_n}{\sum_{i=1}^{n} w_n} \tag{8}$$

$$\sum_{i=1}^{n} W_n = 1$$

Table 2. Classification of groundwater quality based on WQI.

WQI	Type of Water	Classe
0 - 25	Excellent water	A
25.1 - 50	Good water	B
50.1 - 75	Poor water	C
75.1 - 100	Very poor water	D
>100	Water unfit for human consumption	E

Water quality is classified into five (5) categories (Aljanabi et al., 2023; Bindu et al., 2023; Machireddy et al., 2023): excellent, good, poor, very poor, and unfit for human consumption (Table 2).

4. Results and Discussion

4.1. Groundwater Chemical Characteristics

Descriptive statistics for the physicochemical parameters are represented in Table 3. The pH values range from 6.89 to 8.2 with a median value of 7.8, indicating that the water is neutral to slightly alkaline. In the study area, all pH values are within the acceptable pH limits set by the WHO (2017; 2022). Electrical conductivity is the ability of an aqueous solution to conduct electrical current (Marandi et al., 2013) and is an important parameter for assessing water quality (Tutmez et al., 2006). It provides information on the ionic concentration of water. In this study, electrical conductivity ranged from 127 to 5800 µS/cm, with an average of 1524.4 µS/cm and a median of 1107 µS/cm. Approximately 26% of water samples exceeded the WHO permissible limit of 1500 µS/cm. TDS values range from 85.1 mg/L to 3886 mg/L, with average and median values of 1021.4 mg/L and 741.7 mg/L, respectively. Around 26% of water samples exceed the WHO limit. Chloride concentrations in water range from 17.5 to 1556 mg/L, with mean and median values of 267.3 mg/L and 129 mg/L, respectively. NO_3^- content varies from 0.5 to 425 mg/L, with an average of 54.6 mg/L and a median of 24.2 mg/L. Sulfate concentrations range from 1.8 to 587 mg/L, with mean and median values of 69.6 mg/L and 37.6 mg/L, respectively. HCO_3^- concentrations range from 18.3 to 457.5 mg/L, with mean and median values of 330.5 mg/L and 366 mg/L, respectively. Ca^{2+} varied from 13.5 to 353 mg/L, with mean and median values of 105.5 mg/L and 79.1 mg/L, respectively. Magnesium (Mg^{2+}) concentrations range from 0.7 to 188 mg/L, with mean and median values of 44.8 mg/L and 45.5 mg/L. For Na^+ and K^+ ions, their concentration ranges vary from 13.4 to 609.4 mg/L and 0.1 to 23 mg/L, respectively, with associated mean and median values of 116.4 mg/L and 65.8 mg/L for sodium, and 4.7 mg/L and 2.3 mg/L for potassium. The order of abundance of ions in groundwater is defined as follows: $HCO_3^- > Cl^- > SO_4^{2-} > NO_3^-$ for anions, $Na^+ > Ca^{2+} > Mg^{2+} > K^+$ for cations.

Table 3. Descriptive statistics of physicochemical parameters.

Parameters	Units	Moy	Min	Max	Med	Standard Deviation	CV (%)	Permissible Limits of Drinking Water (WHO, 2017)	Percent of Samples Exceeding the Permissible Limits
pH	(-)	7.8	6.9	8.2	7.8	7.8	3.41	6.5 - 8.5	Nil
CE	µS/cm	1524.4	127	5800	1107	1295.3	84.97	1500	26%
TDS	mg/L	1021.4	85.1	3886	741.7	867.9	84.96	1000	26%
Ca^{2+}	mg/L	105.5	13.5	353	79.1	80.7	76.46	75	59%
Mg^{2+}	mg/L	44.8	0.7	188	45.5	36.3	80.92	50	42%

Continued

Na^+	mg/L	116.4	13.4	609.4	65.8	137.7	118.29	200	15%
K^+	mg/L	4.7	0.1	23	2.3	5.6	120.81	12	10%
HCO_3^-	mg/L	330.5	18.3	457.5	366	102.4	30.99	500	Nil
SO_4^{2-}	mg/L	69.6	1.8	587	37.6	106.6	153.25	250	8%
NO_3^-	mg/L	54.8	0.5	425	24.2	90.2	164.67	50	28%
Cl^-	mg/L	267.3	17.5	1556	129	358.7	134.20	250	28%
F^-	mg/L	3.16	0.05	8.4	2.5	2.6	69	1.5	67%

4.2. Hydrochemical Facies

Determining the chemical facies of water is an essential step in understanding and identifying the geological and geochemical factors that influence the hydrogeochemical characteristics of groundwater (Jolaosho et al., 2024). The Piper trilinear diagram reveals four main hydrochemical facies that together describe the evolutionary trends of groundwater in the study area. The Ca-HCO_3 type is dominant (54% of samples) and characterizes wells and boreholes tapping relatively less mineralized waters, typically associated with recharge areas or shorter residence times in carbonate-rich strata. Mixed Ca-Mg-Cl waters (26%) and Ca-Cl waters (10%) represent more evolved compositions, indicative of enhanced interaction with the aquifer matrix and progressive salinization along flow paths.

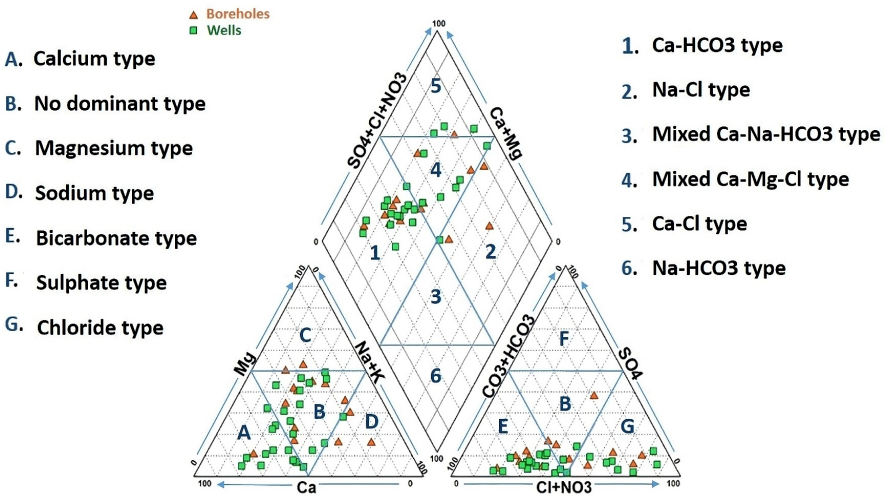

Figure 3. Piper trilinear diagram of groundwater samples.

Na-Cl waters account for 10% of the samples and mark locally more saline conditions, which may result from a combination of halite dissolution, ion exchange, and, in some sectors, the influence of older, more stagnant groundwater (Figure 3). The transition from the Ca-HCO_3 facies found in recharge areas to the mixed Ca-Mg-Cl facies may be related to the dissolution of carbonate rock minerals (calcite, dolomite) and/or the alteration of silicates during water infiltration or along

the flow paths. The occurrence of the mixed Ca-Mg-Cl facies in this study may be associated with a mixing phenomenon observed in areas where rock dissolution is combined with the diffusion of brackish water. This mixed Ca-Mg-Cl facies changes to a Na-Cl facies in certain areas, particularly near the sea. This transition to the Na-Cl facies may be due to the ion exchange process that occurs during marine intrusion, but also to the evaporation process in areas where the aquifer is shallow. The coexistence of these four facies within a relatively small area suggests that the aquifer system is hydrogeochemically heterogeneous, reflecting the superposition of shallow and deep flow systems, lithological variability, and spatially variable anthropogenic inputs.

4.3. Mechanisms Controlling Groundwater Quality

The main natural processes that may lead to variations in the chemical composition of water are evaporation, precipitation, and water-rock interaction (Marandi & Shand, 2018), which are often determined using the Gibbs diagram (1970). The Gibbs diagram highlights the relationship between total dissolved solids (TDS) and the ratio $\left(Cl^{-}/\left(Cl^{-}+HCO_3^{-}\right)\right)$ firstly and the ratio $\left(Na^{+}/\left(Na^{+}+Ca^{2+}\right)\right)$ secondly. This diagram is widely used in numerous studies (Kumar Singh et al., 2013; Li et al., 2016; Sivakarun et al., 2020; Subba Rao et al., 2021) around the world in different geological environments to identify the main natural factors controlling water mineralization. In this study, the plot of chemical data on the Gibbs diagram shows that the majority of water samples (74%) are located within the water-rock interaction zone (**Figure 4**), suggesting possible mineral dissolution through chemical weathering (Ribinu et al., 2023). However, 23% of the samples are located in the evaporation zone, indicating an influence of this process on water chemistry (**Figure 4**). Thus, it may be argued that water-rock interaction is the primary mechanism governing the variation in groundwater chemical composition, followed by evaporation as the secondary mechanism.

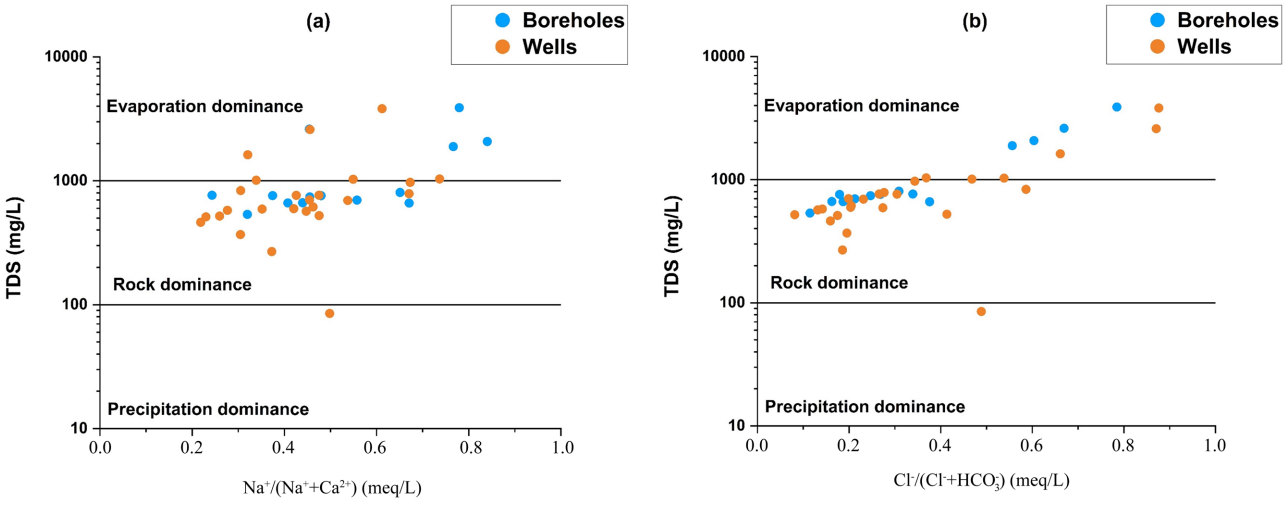

Figure 4. Gibbs plot for mechanisms controlling groundwater chemistry.

Bivariate Diagram

Relationships between major ions are often used to understand hydrogeochemical evolution processes and the mechanisms controlling groundwater chemistry (Zhang et al., 2020). Mineral dissolution is an important process in aquifers that can lead to changes in the chemical composition of groundwater. For example, the dissolution of halite leads to an equivalent release of Na^+ and Cl^- into groundwater (Zhang et al., 2020). When halite dissolution occurs, the points lie on the 1:1 line on the Na^+ vs. Cl^- graph. If the points on the Na^+ vs. Cl^- graph are above the 1:1 line, this indicates an excess of Na^+, which may result from silicate weathering or the base ion exchange process between Na^+ and Ca^{2+} or Mg^{2+} (Sajil Kumar & James, 2016; Zhang et al., 2020). However, if the points lie below the 1:1 line, this indicates chloride enrichment in the water, which may be due to natural phenomena such as marine intrusion (Diongue et al., 2022) or anthropogenic pollution. **Figure 5** shows that most points lie below the 1:1 line, suggesting a sodium deficit relative to chloride. However, some points lie on the 1:1 line, indicating equal concentrations of sodium and chloride in the water, which could result from the dissolution of halite. Some points lie slightly above the 1:1 line, indicating an excess of sodium in the water relative to chloride, which could be related to ion exchange processes or silicate weathering.

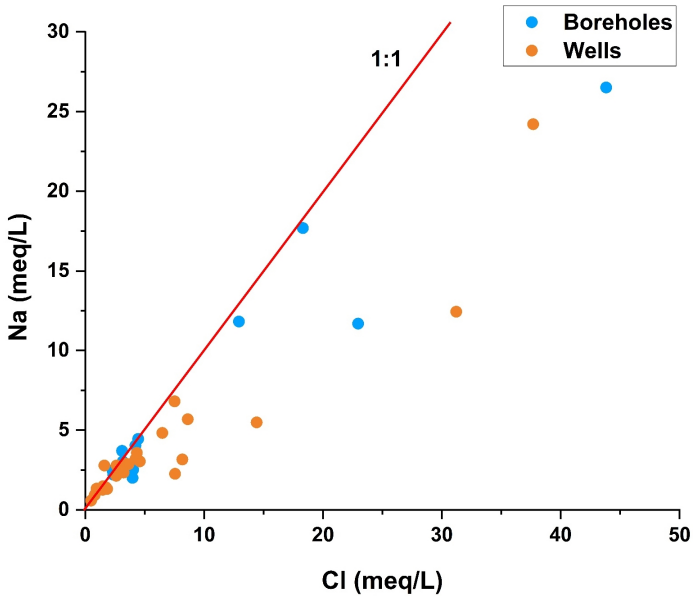

Figure 5. Binary diagram Na^+ vs Cl^-.

Ion Exchange

Ion exchange is a significant process that can alter the chemical composition of groundwater (Zhang et al., 2018). In order to assess the ion exchange process, the bivariate diagram $((Ca + Mg) - (HCO_3 + SO_4))$ vs. $((Na + K) - Cl)$ is commonly used. If ion exchange plays an important role, then a linear relationship with a slope of −1 is observed between the parameters. In this study, **Figure 6** shows that

the majority of points lie on or near a straight line with equation y = −0.9343x − 0.2034 with a slope of −0.93, which is very close to −1, and a correlation coefficient of r^2 = 0.85. This observation suggests that the ion exchange process is important and plays a crucial role in controlling the variation in the chemical composition of groundwater.

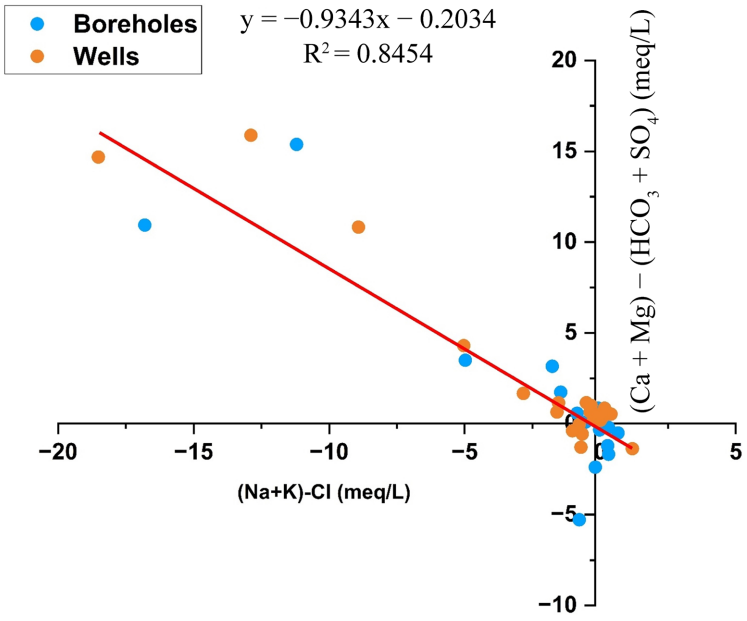

Figure 6. ((Ca + Mg) − (HCO_3 + SO_4)) vs ((Na + K) − Cl).

The influence of the ion exchange process was also checked by calculating the chlorine-alkaline indices (CAI). These are important tools commonly used to evaluate ion exchange reactions between groundwater and the aquifer matrix (Zaidi et al., 2015). Ion exchanges are described by reactions 9 and 10, while ion exchange indices are calculated using Equations (11) and (12) (Zhang et al., 2020).

$$2NaX + Ca^{+} \Leftrightarrow 2Na^{+} + 2CaX_2 \quad \text{(Direct Ion Exchange)} \tag{9}$$

$$CaX_2 + 2Na^{+} \Leftrightarrow 2NaX + Ca^{2+} \quad \text{(Reverse Ion Exchange)} \tag{10}$$

$$CAI-1 = \frac{CL-(Na+K)}{Cl} \tag{11}$$

$$CAI-2 = \frac{CL-(Na+K)}{SO_4 + HCO_3 + CO_3 + NO_3} \tag{12}$$

If CAI > 0, this indicates reverse ion exchange, where Na^+ and K^+ ions present in groundwater are trapped by the aquifer matrix, while Ca^{2+} and Mg^{2+} ions are released into the groundwater. Conversely, if CAI < 0, this indicates direct ion exchange, where Na^+ and K^+ ions are released into the water while Ca^{2+} and Mg^{2+} ions are fixed to the matrix (Brindha et al., 2017; Patel et al., 2023).

In this study, 77% of groundwater samples displayed positive CAI, indicating reverse ion exchange where K^+ and Na^+ ions are fixed by the aquifer matrix while

Ca^{2+} and Mg^{2+} ions are released into the groundwater. In contrast, 23% of the samples showed negative CAI, indicating direct ion exchange where the matrix fixes Ca^{2+} and Mg^{2+} ions and releases Na^{+} and K^{+} ions. These observations suggest that the reverse ion exchange process predominates in the groundwater of the study area (Figure 7).

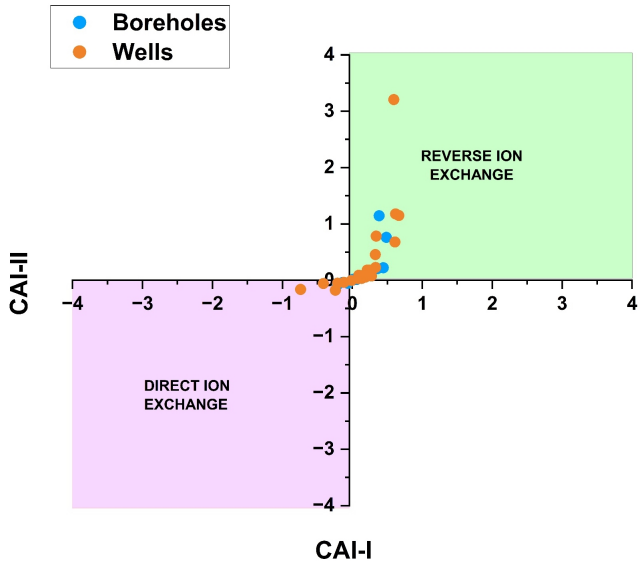

Figure 7. Chloro-alkaline indices diagram CAI-I vs CAI-II.

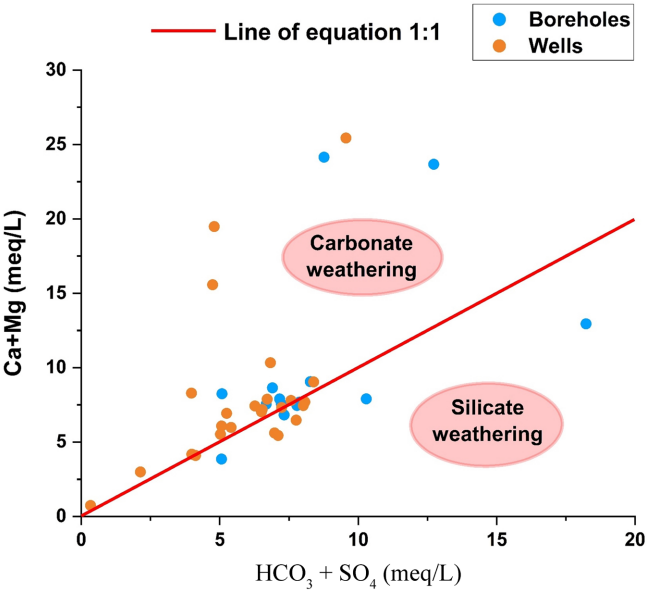

Figure 8. (Ca + Mg) vs (HCO_3 + SO_4).

Weathering of carbonate, silicate, and sulfide minerals and dissolution of evaporites are commonly the main lithogenic sources of ions in water. The binary diagram (Ca + Mg) versus (HCO_3 + SO_4) can be used to study the relative importance of ion exchange and weathering processes (Krishnaraj et al., 2011). This relation-

ship highlights the relative contributions of calcium, magnesium, bicarbonate, and sulfate ions to the chemical composition of groundwater (Mclean et al., 2000). **Figure 8** shows that most samples fall above and around the 1:1 line, indicating that, in addition to the weathering of carbonate minerals, the excess Ca^{2+} and Mg^{2+} in groundwater could be related to the reverse ion exchange process. However, some samples lie below the 1:1 line, suggesting that silicate weathering also contributes to the variation in the chemical composition of groundwater.

Saturation Index

The extent to which water-rock interactions influence the chemical composition of groundwater depends on the magnitude of mineral dissolution and precipitation phenomena, which are determined by the saturation index (SI) (Li et al., 2013). The SI is an essential parameter in geochemistry that describes the quantitative deviation of water from the equilibrium of a specific dissolved mineral (Nandimandalam, 2012; Hussien and Faiyad, 2016). Widely used in the study of geochemical processes, the saturation index is determined using Equation (13) (Kumar Singh et al., 2013; Zhang et al., 2020).

$$SI = \log \frac{K_{IAP}}{K_{SP}} \tag{13}$$

where K_{IAP} represents the ionic activity product for a mineral and K_{SP} is the solubility product constant for the mineral.

When IS < 0, this indicates a solution that is undersaturated with respect to the mineral, promoting its dissolution. Conversely, if IS > 0, this indicates a solution that is supersaturated with respect to the mineral, and precipitation prevails. When IS = 0, this means that the mineral is in equilibrium with the solution (Zhang et al., 2020). In this study, PHREEQC software was used to calculate saturation indices. Owing to the geological context of the study area, which is mainly composed of limestone and marl-limestone, the dissolution of these rocks may be the main source of groundwater mineralization. Bicarbonates in groundwater generally originate from the dissolution of carbonate minerals in aquifers (Anjali et al., 2023). The dissolution of carbonate minerals is described by Equations (14) - (16) (Li et al., 2016; Madioune, 2012).

$$CO_2 + H_2O + CaCO_3 \Leftrightarrow Ca^{2+} + 2HCO_3^- : \text{Calcite Dissolution} \tag{14}$$

$$CO_2 + H_2O + CaMgCO_3 \Leftrightarrow Ca^{2+} + Mg^{2+} + 2HCO_3^- : \text{Dolomit Dissolution} \tag{15}$$

$$CO_2 + H_2O \Leftrightarrow H_2CO_3 \Leftrightarrow HCO_3^- + H^+ : \text{Carbonate Hydrolysis} \tag{16}$$

Results of the saturation index calculations are presented in **Table 4**.

Saturation indices (SI), calculated with respect to calcite, dolomite, halite, and fluorite, further constrain the extent of dissolution and precipitation processes. Mean SI values for calcite (3.15), dolomite (5.97), and fluorite (2.48) are positive, indicating that groundwater is generally supersaturated with respect to these minerals and that precipitation or partial equilibrium conditions are likely to occur along flow paths. In contrast, halite exhibits a negative mean SI (−3.88), consistent with persistent undersaturation and ongoing dissolution where halite is present

in the geological formations.

Given the carbonate dominated lithology of the study area, these results are consistent with an initial phase of carbonate dissolution during recharge, followed by a progressive approach to equilibrium and local precipitation of calcite and dolomite in more evolved waters. The supersaturation with respect to fluorite suggests that fluoride concentrations in groundwater are controlled by complex interactions among fluorite dissolution-precipitation, pH-dependent sorption-desorption reactions, and competition with other anions such as bicarbonate and hydroxide.

Table 4. Statistics of mineral saturation index.

Saturation Index of Minerals	N	Min	Max	Mean
Calcite	39	0.9	3.79	3.15
Dolomite	39	0.67	7.54	5.97
Halite	39	−5.39	−1.98	−3.88
Fluorite	39	−0.21	3.41	2.48

4.4. Water Quality Index (WQI)

Results of the water quality index are shown in **Table 5**. These results show that the majority of groundwater samples (64%) (F2, F4 - F6, F8 - F10, F12, F14 - F16, F18, P1, P6 - P10, P17, P18, P21, P23, P24, P26, and P27) are unfit for human consumption (class E). However, 10% of the groundwater samples (P2, P14, P15, and P16) had excellent water quality (class A); 13% of the groundwater samples (F1, F3, P11, P20, and P25) had good water quality (class B); 5% of groundwater samples (P4 and P2) have poor water quality (class C); 8% of groundwater samples (P3, P5, and P22) have very poor water quality (class D).

Spatial distribution of water quality indices (**Figure 9**) shows that unsuitable water for human consumption is spread across the entire study area, with the exception of certain parts, particularly in the northwest, south, and at certain locations such as Keur Yerim (P2), Ndiol Khokhane (P11) and Roff (P25), where the water is of excellent quality and good quality, respectively, for the latter two points. In the area, the decline in water quality is mainly linked to the high fluoride concentrations recorded in several localities and, to a certain extent, to nitrate concentrations, which can have adverse effects on human health. In fact, consuming water polluted with nitrate can lead to diseases such as methemoglobinemia, thyroid problems, and cancer (Martínez et al., 2017; Tokazhanov et al., 2020), while consuming water polluted with fluoride can cause dental and skeletal damage (Pramanik & Saha, 2017). In addition, the high proportion of samples falling into the "unfit for drinking" class is comparable to results obtained in other semi-arid basins (Ibn Ali et al., 2020; Khadija et al., 2021; Zhang et al., 2021) where WQI is used to evaluate groundwater quality, although the relative contribution of each

ion may differ depending on land use and lithology. This underlines the need to not only report WQI values, but also to interpret them in the light of the underlying hydrogeochemical processes and human pressures.

Table 5. Classification of groundwater samples based on water quality index.

Range of WQI	Type of Water Quality	Classe	Number of Samples	% Samples
0 - 25	Excellent water quality	A	4	10
25.1 - 50	Good water quality	B	5	13
50.1 - 75	Poor water quality	C	2	5
75.1 - 100	Very poor water quality	D	3	8
>100	Unfit water for human consumption	E	25	64
			39	**100**

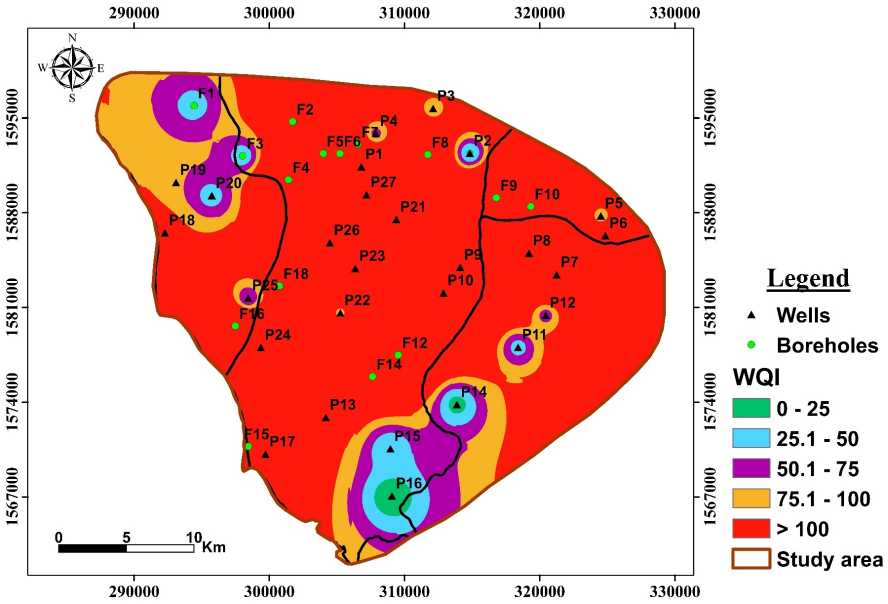

Figure 9. Spatial distribution of water quality index in the study area.

4.5. Multivariate Statistical Analysis

Correlation Analysis of Physicochemical Parameters

Pearson's correlation analysis (Figure 10) highlights strong, statistically significant positive correlations between EC, TDS, and most major ions, confirming that these species jointly contribute to groundwater mineralization. In particular, EC correlates strongly with Cl^-, Na^+, Ca^{2+}, Mg^{2+}, SO_4^{2-}, NO_3^- and K^+, underlining that increases in salinity reflect both natural water-rock interaction and anthropogenic inputs. A very strong correlation between pH and HCO_3^- indicates that bicarbonate is the main driver of groundwater alkalinity and suggests extensive carbonate dissolution and CO_2^- water interactions in the unsaturated and

saturated zones. This alkalinity promotes fluoride enrichment in groundwater (Adimalla et al., 2019), as evidenced by the positive correlations between F^- and pH ($r = 0.61$; $p < 0.001$), as well as F^- and HCO_3^- ($r = 0.67$; $p < 0.001$). There is also a strong positive correlation between Na^+ and Cl^- concentrations ($r = 0.95$; $p < 0.001$). This association suggests a common origin for these two ions in groundwater (Sajil Kumar & James, 2016). Furthermore, the negative correlation between calcium (Ca^{2+}) and bicarbonates (HCO_3^-) ($r = -0.21$; $p > 0.05$) suggests that calcite ($CaCO_3$) is not the main source of Ca^{2+} in groundwater. Bicarbonates could result from the dissolution of carbonate rocks by carbon dioxide (CO_2) rich waters. The positive correlation between nitrate (NO_3^-) and calcium (Ca^{2+}) ($r = 0.62$; $p < 0.001$), as well as between nitrate and chloride ($r = 0.66$; $p < 0.001$), indicates a possible anthropogenic origin linked to agricultural activities or domestic waste (Torres-Martínez et al., 2021). Finally, the positive correlation between sodium (Na^+) and potassium (K^+) ($r = 0.84$; $p < 0.001$) suggests a possible common origin for these ions, which could be related to silicate weathering (Refat Nasher & Humayan Ahmed, 2021). Potassium (K^+) is significantly correlated with chloride Cl^- ($r = 0.75$; $p < 0.001$), indicating that a higher concentration of K^+ can lead to an increase in chloride concentration (Ekbal & Khan, 2022).

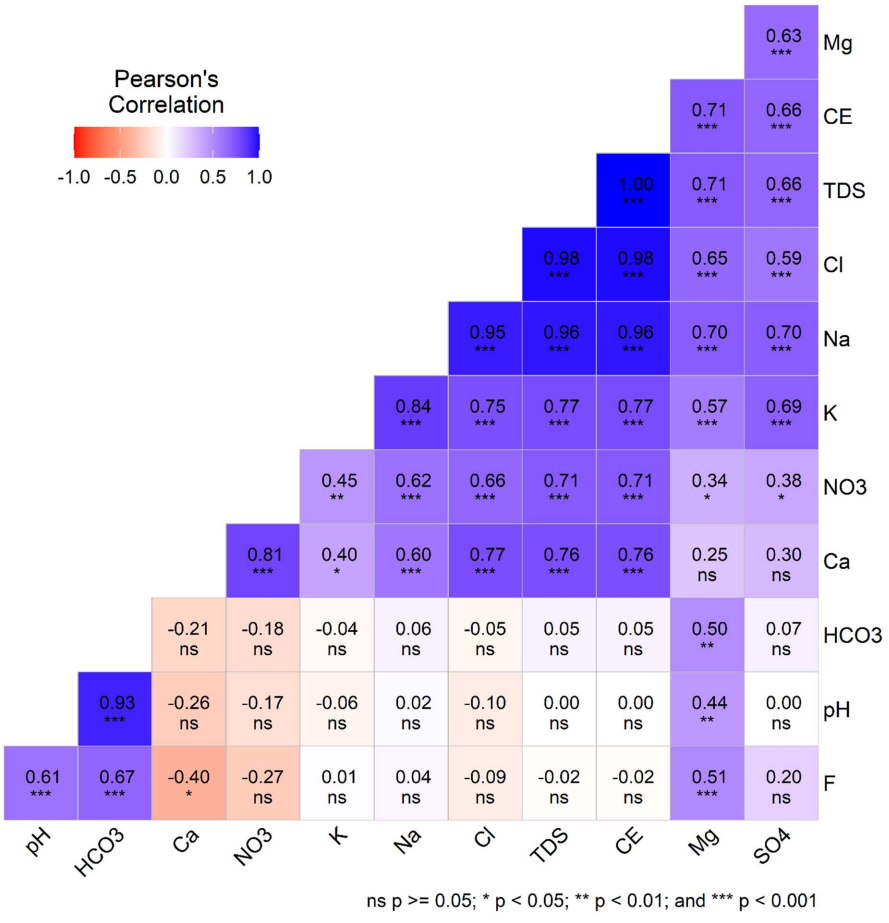

Figure 10. Pearson correlation matrix of physicochemical parameters.

Principal Component Analysis

PCA extracted two principal components with eigenvalues greater than 1, together explaining 80.54% of the total variance in the dataset, thereby providing a compact yet robust representation of the controlling processes. The results of the principal component analysis are presented in Table 6, which shows the eigenvalues, variances, and cumulative variances. The first component (PC1) shows high positive loadings on EC, TDS, Na^+, Cl^-, Ca^{2+}, Mg^{2+}, SO_4^{2-} and NO_3^-, and can be interpreted as a "mineralization-anthropogenic" factor that integrates both natural salinities built up and superimposed contamination by nitrate and other ions of anthropogenic origin. The second component (PC2), with strong loadings on pH, HCO_3^- and F^-, represents an "alkalinity-fluoride" factor, specifically discriminating fluoride-rich, alkaline waters from the rest of the dataset (Figures 11-13). Alkalinity, which is linked to the bicarbonate enrichment of water, promotes anion exchange between F^- and OH^-, with the release of F^- and the fixation of OH^- in the aquifer matrix, thereby leading to an increase in fluoride concentration. This explains the strong positive correlation between pH and fluoride, but also between F^- and HCO_3^-.

Table 6. Eigenvalues, variance and cumulative variance of the selected components.

Principle Component	Eigenvalues	Variance (%)	Cumulative Variance (%)
1	6.63	55.27	55.27
2	3.03	25.27	80.54

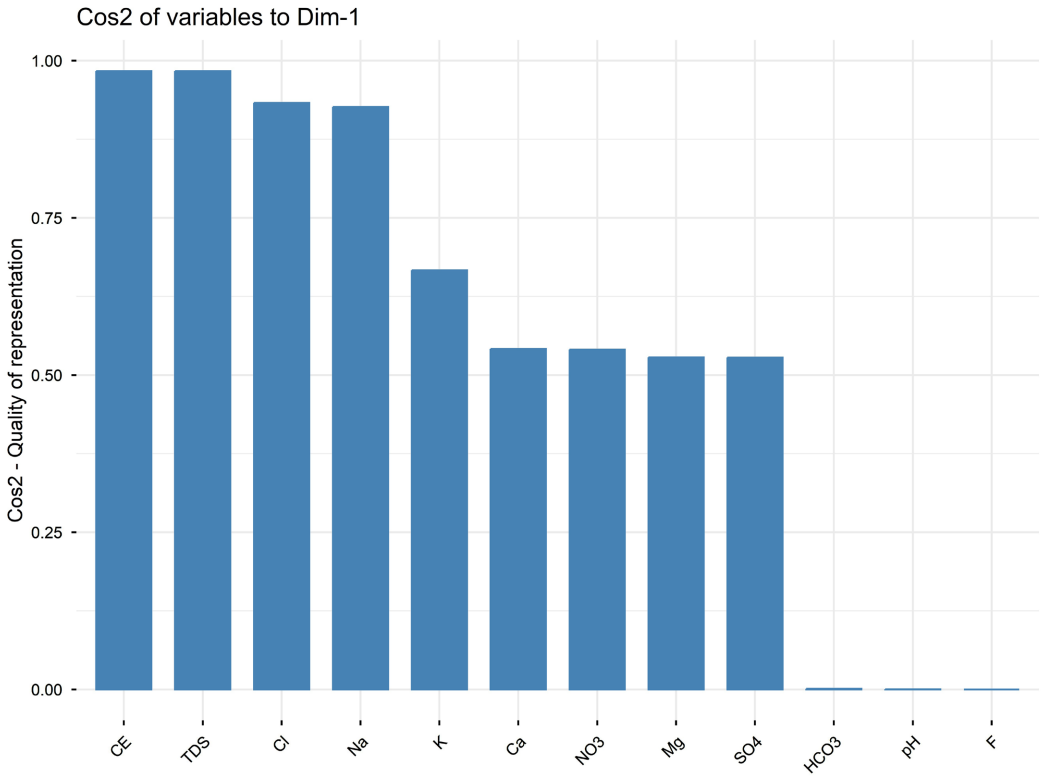

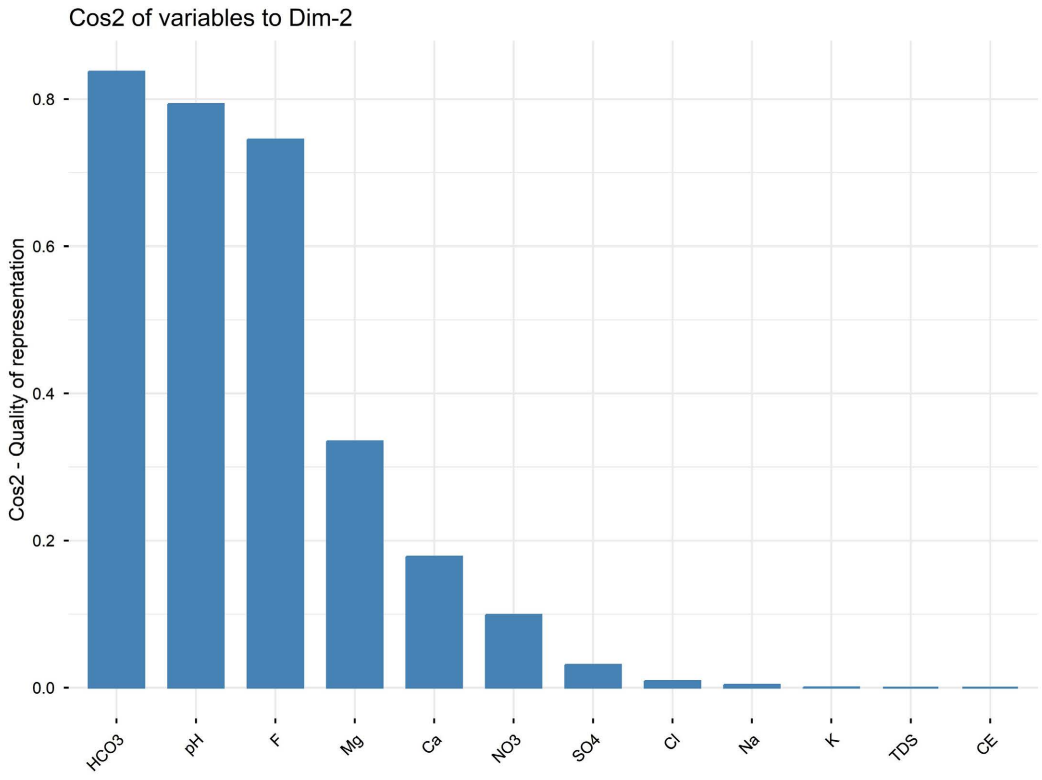

Figure 11. Variables' contribution to the first two principal components.

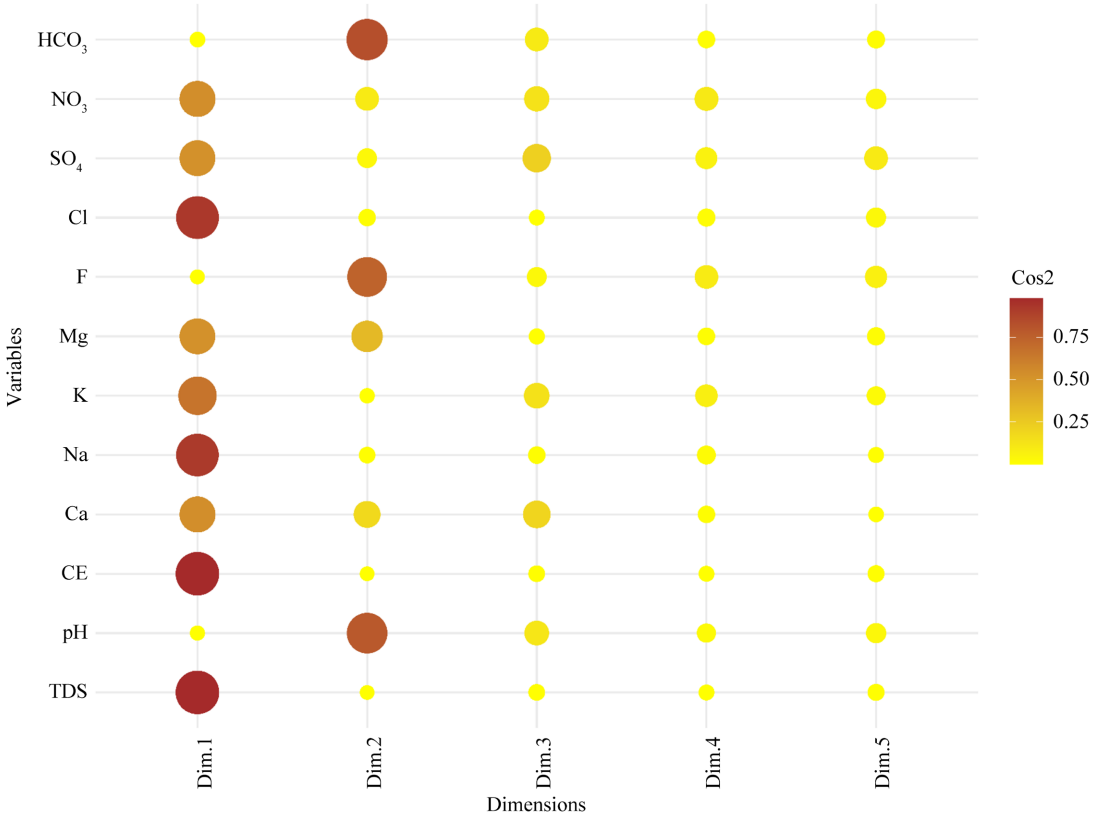

Figure 12. Correlation matrix between variables and principal components.

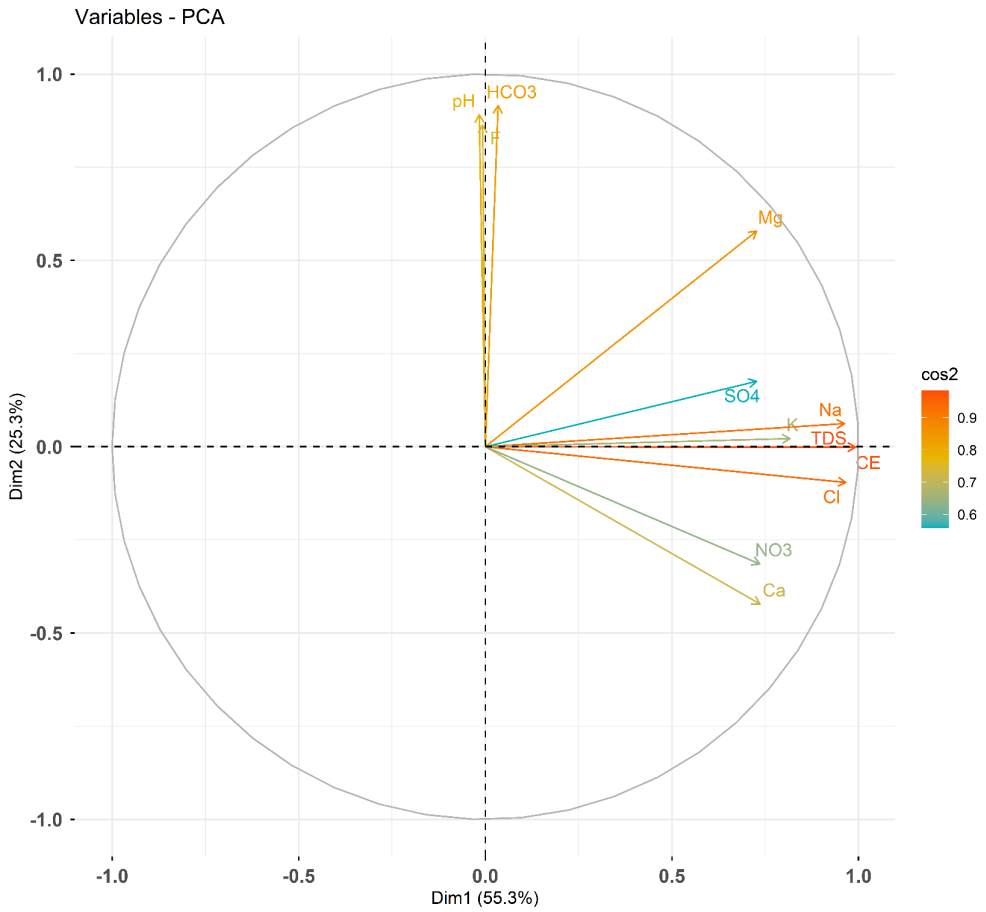

Figure 13. Variables projection on the factorial plane (Dim1 - Dim2).

Hierarchical Cluster Analysis

Hierarchical cluster analysis classifies water samples into two (2) distinct clusters based on their chemical characteristics. Cluster 1: includes boreholes F12, F15, F16, F18, P15, P18, and well P22 (Figure 14) and represents 18% of groundwater samples. It is characterized by highly mineralized water with high average values for TDS (2642.5 mg/L), electrical conductivity (3944 µS/cm), sodium (361 mg/L), chloride (919.7 mg/L), calcium (231.2 mg/L), sulfate (222.3 mg/L), and nitrate (180.6 mg/L) (Table 7). These chemical parameters, combined with TDS and electrical conductivity (EC), reveal that cluster 1 is linked to groundwater mineralization, which may result from natural processes such as water-rock interaction, but also from anthropogenic pollution.

Cluster 2: includes boreholes F1 - F6, F8 - F10, F14, and wells P1 - P12, P14, P16, P17, P20, P21, P23 - P27, and represents 82% of water samples (Figure 14). Cluster 2 is associated with moderately mineralized, alkaline waters with a dominant mixed HCO_3^- facies. It includes water samples whose physicochemical parameters have lower average values than those in cluster 1, with the exception of bicarbonates, fluoride, and pH, which have average values of 332.8 mg/L, 3.2 mg/L, and 7.8 mg/L, respectively (Table 7).

Table 7. Physicochemical characteristics of each cluster.

Water Type	Cluster 1	Cluster 2
	Brackish	Fresh
Dominant Facies Type	Mixte-Cl	Mixte-HCO_3
TDS	2642.5	666.7
pH	7.7	7.8
CE	3944	995.1
Ca	231.2	78
Na	361	62.9
K	12.4	3
Mg	86.2	35.8
F	2.8	3.2
Cl	919.7	124.6
SO_4	222.3	36.2
NO_3	180.6	27.2
HCO_3	319.8	332.8

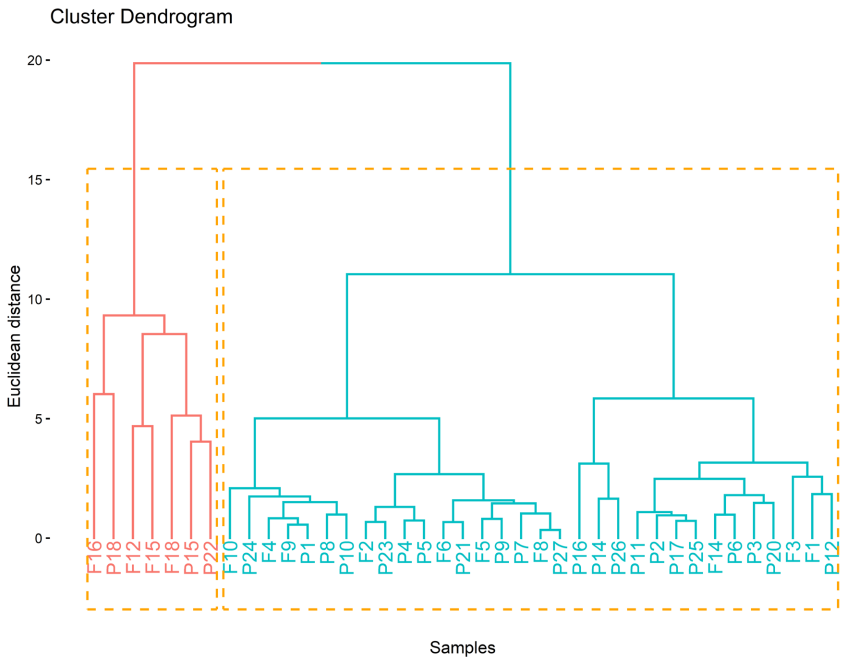

Figure 14. Dendrogram generated through hierarchical cluster analysis of groundwater samples.

5. Conclusion

Groundwater is a vital resource in the Mbour-Fatick area, where the scarcity of surface water and rapid socioeconomic development have led to an increasing reliance on wells and boreholes for domestic, agricultural, and touristic uses. In this

context, a combined hydrogeochemical and statistical approach was applied to 39 groundwater samples collected in 2023 to characterize water chemistry, identify the main controlling processes, and evaluate groundwater suitability for drinking purposes.

Groundwater is mainly neutral to slightly alkaline and is dominated by Ca-HCO_3, mixed Ca-Mg-Cl, Na-Cl, and Ca-Cl facies, reflecting the influence of carbonate and marl-limestone formations and variable contributions of evaporitic and marine-derived ions. Hydrogeochemical diagrams, saturation indices, and chloro-alkaline indices show that water-rock interaction, base ion exchange, and evaporation are the dominant processes controlling mineralization, with reverse ion exchange playing a major role in the release of Ca^{2+} and Mg^{2+} to groundwater.

The water quality index, calculated from eleven physicochemical parameters, indicates that 64% of groundwater samples are unfit for human consumption, mainly due to fluoride and nitrate concentrations exceeding the World Health Organization guideline values in 66% and 28% of samples, respectively. Principal component analysis reveals two main components explaining 80.54% of the total variance: the first is associated with overall mineralization and anthropogenic inputs, whereas the second is controlled by alkalinity and fluoride enrichment, confirming the dual influence of natural and human-related processes. Hierarchical cluster analysis separates highly mineralized, nitrate- and chloride-rich brackish waters from moderately mineralized alkaline waters, providing a useful framework for spatially prioritizing monitoring and mitigation actions.

These findings highlight an urgent need to strengthen groundwater management in the Mbour-Fatick area by: 1) protecting recharge zones from agricultural and domestic pollution, 2) promoting low-cost defluorination and nitrate-removal options for the most affected localities, and 3) integrating groundwater quality criteria into regional planning and drinking water supply programs. Future work should address seasonal variability, include additional parameters such as trace metals and microbiological indicators, and explore advanced water quality indices or modelling tools to better capture the complexity of groundwater evolution in this semi-arid coastal setting.

Acknowledgements

The authors are thankful to the Geo-Environment Laboratory of the University of Lille in France, which performed the chemical analysis, and to the anonymous reviewers for their valuable suggestions and useful comments to improve the quality of this paper.

Conflicts of Interest

The authors declare no conflicts of interest regarding the publication of this paper.

References

Adimalla, N., & Venkatayogi, S. (2018). Geochemical Characterization and Evaluation of

Groundwater Suitability for Domestic and Agricultural Utility in Semi-Arid Region of Basara, Telangana State, South India. *Applied Water Science, 8,* Article No. 44. https://doi.org/10.1007/s13201-018-0682-1

Adimalla, N., Venkatayogi, S., & Das, S. V. G. (2019). Assessment of Fluoride Contamination and Distribution: A Case Study from a Rural Part of Andhra Pradesh, India. *Applied Water Science, 9,* Article No. 94. https://doi.org/10.1007/s13201-019-0968-y

Alfaleh, A., Ben Khedher, N., & Alviz-Meza, A. (2023). Is the Entropy-Weighted Water Quality Index a Suitable Index for Evaluating the Groundwater Quality in Ha'il, Saudi Arabia? *Water Science & Technology, 88,* 778-797. https://doi.org/10.2166/wst.2023.230

Aljanabi, Z. Z., Al-Obaidy, A. M. J., & Hassan, F. M. (2023). A Novel Water Quality Index for Iraqi Surface Water. *Baghdad Science Journal, 20,* Article 50. https://doi.org/10.21123/bsj.2023.9348

Ani, M., Jaunat, J., Marin, B., Huneau, F., & Gnandi, K. (2024). Origin and Mineralization Processes of Groundwater in Metamorphic Hardrock Aquifers in West Africa: Insights from Stable Isotopes (δ^2H and δ^{18}O) and Major Ions. In *EGU General Assembly 2024* (pp. EGU24-18288). https://doi.org/10.5194/egusphere-egu24-18288

Anjali, R., Krishnakumar, S., Thivya, C., Kasilingam, K., Suresh Gandhi, M., Selvakumar, S. et al. (2023). Assessment of Mine Water Quality for Domestic and Irrigation Purposes, Neyveli Coal Mine Region, Southern India. *Total Environment Research Themes, 6,* Article ID: 100047. https://doi.org/10.1016/j.totert.2023.100047

Bindu, O. S. D. H., Gayathri, V., Swaranya, T., & Vyshnavi, J. (2023). Assessment of Ground Water Quality Using Water Quality Index and Gis. *E3S Web of Conferences, 391,* Article ID: 01208. https://doi.org/10.1051/e3sconf/202339101208

Bodrud-Doza, M., Islam, A. R. M. T., Ahmed, F., Das, S., Saha, N., & Rahman, M. S. (2016). Characterization of Groundwater Quality Using Water Evaluation Indices, Multivariate Statistics and Geostatistics in Central Bangladesh. *Water Science, 30,* 19-40. https://doi.org/10.1016/j.wsj.2016.05.001

Brindha, K., Pavelic, P., Sotoukee, T., Douangsavanh, S., & Elango, L. (2017). Geochemical Characteristics and Groundwater Quality in the Vientiane Plain, Laos. *Exposure and Health, 9,* 89-104. https://doi.org/10.1007/s12403-016-0224-8

Chaudhry, A. K., Kumar, K., & Alam, M. A. (2019). Groundwater Contamination Characterization Using Multivariate Statistical Analysis and Geostatistical Method. *Water Supply, 19,* 2309-2322. https://doi.org/10.2166/ws.2019.111

Chen, C., Holyoak, M., Wang, Y., Si, X., & Ding, P. (2019). Spatiotemporal Distribution of Seasonal Bird Assemblages on Land-Bridge Islands: Linking Dynamic and Static Views of Metacommunities. *Avian Research, 10,* Article No. 25. https://doi.org/10.1186/s40657-019-0164-7

Dhakate, R., More, S., Duvva, L. K., & Enjamuri, S. (2023). Groundwater Chemistry and Health Hazard Risk Valuation of Fluoride and Nitrate Enhanced Groundwater from a Semi-Urban Region of South India. *Environmental Science and Pollution Research, 30,* 43554-43572. https://doi.org/10.1007/s11356-023-25287-z

Diedhiou, M., Ndoye, S., Diagne, A., Gauthier, A., Whonlich, S., Faye, S. et al. (2024). Spatial Distribution and Potential Health Risk Assessment of Fluoride and Nitrate Concentrations in Groundwater from Mbour-Fatick Area, Western Central Senegal. *Journal of Water Resource and Protection, 16,* 695-719. https://doi.org/10.4236/jwarp.2024.1611039

Diongue, D. M. L., Sagnane, L., Emvoutou, H., Faye, M., Gueye, I. D., & Faye, S. (2022). Evaluation of Groundwater Quality in the Deep Maastrichtian Aquifer of Senegal Using Multivariate Statistics and Water Quality Index-Based Gis. *Journal of Environmental*

Protection, 13, 819-841. https://doi.org/10.4236/jep.2022.1311052

Diop, A., Guernet, C., & Poignant, A. (1982). Microfaune du Paléocène de quelques sondages du Dôme du Sénégal occidental; observations sur les Ostracodes. *Geobios, 15,* 19-31. https://doi.org/10.1016/S0016-6995(82)80055-7

Ekbal, E., & Khan, T. A. (2022). Hydrogeochemical Characterization of Groundwater Quality in Parts of Amroha District, Western Uttar Pradesh, India. *HydroResearch, 5,* 54-70. https://doi.org/10.1016/j.hydres.2022.07.002

Fabbrocino, S., Rainieri, C., Paduano, P., & Ricciardi, A. (2019). Cluster Analysis for Groundwater Classification in Multi-Aquifer Systems Based on a Novel Correlation Index. *Journal of Geochemical Exploration, 204,* 90-111. https://doi.org/10.1016/j.gexplo.2019.05.006

Güler, C., Thyne, G. D., McCray, J. E., & Turner, K. A. (2002). Evaluation of Graphical and Multivariate Statistical Methods for Classification of Water Chemistry Data. *Hydrogeology Journal, 10,* 455-474. https://doi.org/10.1007/s10040-002-0196-6

Gulgundi, M. S., & Shetty, A. (2018). Groundwater Quality Assessment of Urban Bengaluru Using Multivariate Statistical Techniques. *Applied Water Science, 8,* Article No. 43. https://doi.org/10.1007/s13201-018-0684-z

Hussien, B. M., & Faiyad, A. S. (2016). Modeling the Hydrogeochemical Processes and Source of Ions in the Groundwater of Aquifers within Kasra-Nukhaib Region (West Iraq). *International Journal of Geosciences, 7,* 1156-1181. https://doi.org/10.4236/ijg.2016.710087

Ibn Ali, Z., Gharbi, A., & Zairi, M. (2020). Evaluation of Groundwater Quality in Intensive Irrigated Zone of Northeastern Tunisia. *Groundwater for Sustainable Development, 11,* Article ID: 100482. https://doi.org/10.1016/j.gsd.2020.100482

Islam, M. M., Lenz, O. K., Azad, A. K., Ara, M. H., Rahman, M., & Hassan, N. (2017). Assessment of Spatio-Temporal Variations in Water Quality of Shailmari River, Khulna (Bangladesh) Using Multivariate Statistical Techniques. *Journal of Geoscience and Environment Protection, 5,* 1-26. https://doi.org/10.4236/gep.2017.51001

Jenn, F., Kofahl, C., Müller, M., Radschinski, J., & Voigt, H. (2007). Interpretation of Geological, Hydrogeological, and Geochemical Results. In K. Knödel, G. Lange, & H. J. Voigt (Eds.), *Environmental Geology* (pp. 941-1051). Springer. https://doi.org/10.1007/978-3-540-74671-3_18

Jiang, Q., Liu, Q., Liu, Y., Zhu, J., Chai, H., & Chen, K. (2023). Chemical Composition of Groundwater and Its Controlling Factors in the Liuzhuang Coal Mine, Northern Anhui Province, China. *Water Supply, 23,* 4937-4956. https://doi.org/10.2166/ws.2023.290

Jolaosho, T. L., Mustapha, A. A., & Hundeyin, S. T. (2024). Hydrogeochemical Evolution and Heavy Metal Characterization of Groundwater from Southwestern, Nigeria: An Integrated Assessment Using Spatial, Indexical, Irrigation, Chemometric, and Health Risk Models. *Heliyon, 10,* e38364. https://doi.org/10.1016/j.heliyon.2024.e38364

Jung, H., Ha, K., Koh, D., Kim, Y., & Lee, J. (2021). Statistical Analysis Relating Variations in Groundwater Level to Droughts on Jeju Island, Korea. *Journal of Hydrology: Regional Studies, 36,* Article ID: 100879. https://doi.org/10.1016/j.ejrh.2021.100879

Khadija, D., Hicham, A., Rida, A., Hicham, E., Nordine, N., & Najlaa, F. (2021). Surface Water Quality Assessment in the Semi-Arid Area by a Combination of Heavy Metal Pollution Indices and Statistical Approaches for Sustainable Management. *Environmental Challenges, 5,* Article ID: 100230. https://doi.org/10.1016/j.envc.2021.100230

Krishnaraj, S., Murugesan, V., K, V., Sabarathinam, C., Paluchamy, A., & Ramachandran, M. (2011). Use of Hydrochemistry and Stable Isotopes as Tools for Groundwater Evolution and Contamination Investigations. *Journal of Geo-sciences, 1,* 16-25. https://doi.org/10.5923/j.geo.20110101.02

Kumar Singh, A., Raj, B., Tiwari, A. K., & Mahato, M. K. (2013). Evaluation of Hydrogeochemical Processes and Groundwater Quality in the Jhansi District of Bundelkhand Region, India. *Environmental Earth Sciences, 70,* 1225-1247. https://doi.org/10.1007/s12665-012-2209-7

Kura, N., Ramli, M., Sulaiman, W., Ibrahim, S., Aris, A., & Mustapha, A. (2013). Evaluation of Factors Influencing the Groundwater Chemistry in a Small Tropical Island of Malaysia. *International Journal of Environmental Research and Public Health, 10,* 1861-1881. https://doi.org/10.3390/ijerph10051861

Li, P., Qian, H., Wu, J., Zhang, Y., & Zhang, H. (2013). Major Ion Chemistry of Shallow Groundwater in the Dongsheng Coalfield, Ordos Basin, China. *Mine Water and the Environment, 32,* 195-206. https://doi.org/10.1007/s10230-013-0234-8

Li, P., Wu, J., & Qian, H. (2016). Hydrochemical Appraisal of Groundwater Quality for Drinking and Irrigation Purposes and the Major Influencing Factors: A Case Study in and around Hua County, China. *Arabian Journal of Geosciences, 9,* Article No. 15. https://doi.org/10.1007/s12517-015-2059-1

Liu, G., Ma, F., Liu, G., Zhao, H., Guo, J., & Cao, J. (2019). Application of Multivariate Statistical Analysis to Identify Water Sources in a Coastal Gold Mine, Shandong, China. *Sustainability, 11,* Article 3345. https://doi.org/10.3390/su11123345

Ma, R., Shi, J., Liu, J., & Gui, C. (2014). Combined Use of Multivariate Statistical Analysis and Hydrochemical Analysis for Groundwater Quality Evolution: A Case Study in North Chain Plain. *Journal of Earth Science, 25,* 587-597. https://doi.org/10.1007/s12583-014-0446-2

Machireddy, S. R., Bhargava, B., & Chennapa, B. (2023). Applications of Geospatial Technology and Water Quality Index in The Assessment of Groundwater Quality. https://doi.org/10.21203/rs.3.rs-3325389/v1

Madioune, H. (2012). *Etude hydrogéologique du système aquifère du horst de Diass en condition d'exploitation intensive (bassin sédimentaire sénégalais): Apport des techniques de télédétection, modélisation, géochimie et isotopie.* Thèse de doctorat, Université de Cheikh Anta Diop de Dakar et Université de Liège.

Marandi, A., & Shand, P. (2018). Groundwater Chemistry and the Gibbs Diagram. *Applied Geochemistry, 97,* 209-212. https://doi.org/10.1016/j.apgeochem.2018.07.009

Marandi, A., Polikarpus, M., & Jõeleht, A. (2013). A New Approach for Describing the Relationship between Electrical Conductivity and Major Anion Concentration in Natural Waters. *Applied Geochemistry, 38,* 103-109. https://doi.org/10.1016/j.apgeochem.2013.09.003

Marghade, D., Malpe, D. B., & Subba Rao, N. (2019). Applications of Geochemical and Multivariate Statistical Approaches for the Evaluation of Groundwater Quality and Human Health Risks in a Semi-Arid Region of Eastern Maharashtra, India. *Environmental Geochemistry and Health, 43,* 683-703. https://doi.org/10.1007/s10653-019-00478-1

Martínez, J., Ortiz, A., & Ortiz, I. (2017). State-of-the-Art and Perspectives of the Catalytic and Electrocatalytic Reduction of Aqueous Nitrates. *Applied Catalysis B: Environmental, 207,* 42-59. https://doi.org/10.1016/j.apcatb.2017.02.016

Mclean, W., Jankowski, J., & Lavitt, N. (2000). Groundwater Quality and Sustainability in an Alluvial Aquifer, Australia. In O. Sililo (Ed.), *Groundwater: Past Achievements and Future Challenges* (pp. 567-573). Taylor & Francis. http://pascal-francis.inist.fr/vibad/index.php?action=getRecordDetail&idt=6178313

Meng, J., Xiao, G., Qi, M., Han, X., Gou, Q., Hao, X. et al. (2024). Comparing Roles of Multiple Contamination Indicators in Tracing Groundwater Pollution Nearby a Typical Municipal Solid Waste (MSW) Landfill. *Heliyon, 10,* e35601.

https://doi.org/10.1016/j.heliyon.2024.e35601

Mohammed, M. A. A., Szabó, N. P., & Szűcs, P. (2022). Multivariate Statistical and Hydrochemical Approaches for Evaluation of Groundwater Quality in North Bahri City-Sudan. *Heliyon, 8,* e11308. https://doi.org/10.1016/j.heliyon.2022.e11308

Monciardini, C. (1966). *La sédimentation éocène au Sénégal*. Mémoire Bureau Recherches Géologiques Minières, No. 43, 65 p.

Nandimandalam, J. R. (2012). Evaluation of Hydrogeochemical Processes in the Pleistocene Aquifers of Middle Ganga Plain, Uttar Pradesh, India. *Environmental Earth Sciences, 65,* 1291-1308. https://doi.org/10.1007/s12665-011-1377-1

Omo-Irabor, O. O., Olobaniyi, S. B., Oduyemi, K., & Akunna, J. (2008). Surface and Groundwater Water Quality Assessment Using Multivariate Analytical Methods: A Case Study of the Western Niger Delta, Nigeria. *Physics and Chemistry of the Earth, Parts A/B/C, 33,* 666-673. https://doi.org/10.1016/j.pce.2008.06.019

Patel, D. D., Mehta, D. J., Azamathulla, H. M., Shaikh, M. M., Jha, S., & Rathnayake, U. (2023). Application of the Weighted Arithmetic Water Quality Index in Assessing Groundwater Quality: A Case Study of the South Gujarat Region. *Water, 15,* Article 3512. https://doi.org/10.3390/w15193512

Pitaud, G. (1980). *Etudes hydrogéologiques des calcaires paléocènes de la région de Mbour. Evaluation des ressources en eau et possibilités d'exploitation* (p. 52). Rapport de Synthèse, Direction Générale de l'hydraulique et de l'Equipement Rural-Direction des Etudes Hydrauliques.

Pramanik, S., & Saha, D. (2017). The Genetic Influence in Fluorosis. *Environmental Toxicology and Pharmacology, 56,* 157-162. https://doi.org/10.1016/j.etap.2017.09.008

Refat Nasher, N. M., & Humayan Ahmed, M. (2021). Groundwater Geochemistry and Hydrogeochemical Processes in the Lower Ganges-Brahmaputra-Meghna River Basin Areas, Bangladesh. *Journal of Asian Earth Sciences: X, 6,* Article ID: 100062. https://doi.org/10.1016/j.jaesx.2021.100062

Ribinu, S. K., Prakash, P., Khan, A. F., Bhaskar, N. P., & Arunkumar, K. S. (2023). Hydrogeochemical Characteristics of Groundwater in Thoothapuzha River Basin, Kerala, South India. *Total Environment Research Themes, 5,* Article ID: 100021. https://doi.org/10.1016/j.totert.2022.100021

Saint-Marc, P., & Sarr, R. (1984). Précisions biostratigraphiques et paléoenvironnementales sur le sommet du Paléocène et la base de l'Eocène de la région de Mbour-Joal (Sénégal). *Journal of African Earth Sciences (1983), 2,* 203-207. https://doi.org/10.1016/s0731-7247(84)80015-4

Sajil Kumar, P. J., & James, E. J. (2016). Identification of Hydrogeochemical Processes in the Coimbatore District, Tamil Nadu, India. *Hydrological Sciences Journal, 61,* 719-731. https://doi.org/10.1080/02626667.2015.1022551

Sajil Kumar, P. J., Jose, A., & James, E. J. (2013). Spatial and Seasonal Variation in Groundwater Quality in Parts of Cuddalore District, South India. *National Academy Science Letters, 36,* 167-179. https://doi.org/10.1007/s40009-013-0115-5

Salehi, S., Chizari, M., Sadighi, H., & Bijani, M. (2018). Assessment of Agricultural Groundwater Users in Iran: A Cultural Environmental Bias. *Hydrogeology Journal, 26,* 285-295. https://doi.org/10.1007/s10040-017-1634-9

Salem, S., Gaagai, A., Ben Slimene, I., Moussa, A., Zouari, K., Yadav, K. et al. (2023). Applying Multivariate Analysis and Machine Learning Approaches to Evaluating Groundwater Quality on the Kairouan Plain, Tunisia. *Water, 15,* Artice 3495. https://doi.org/10.3390/w15193495

Sarr, J. B. J. (2003). *Etudes de minéralisations particulières: Le cas du fluor dans les eaux*

des nappes superficielles de la zone de Mbour-Fatick. Diplôme d'Etudes Approfondies (DEA), Université Cheikh Anta Diop de Dakar, 57 p. http://196.1.97.20/viewer.php?c=mmoires&d=mems%5f2658

Sarr, R. (1982). *Etude hydrogéologique de la région de Joal-Fadiouth (Sénégal).* Ph.D. Thesis, Université Cheikh Anta Diop de Dakar, 192 p.

Sarr, R. (1999). Le Paléogène de la région de Mbour-Joal (Sénégal occidental): Biostratigraphie, étude systématique des ostracodes, paleoenvironnement. *Revue de Paléobiologie, 18,* 1-29.

Seifi, A., Dehghani, M., & Singh, V. P. (2020). Uncertainty Analysis of Water Quality Index (WQI) for Groundwater Quality Evaluation: Application of Monte-Carlo Method for Weight Allocation. *Ecological Indicators, 117,* Article ID: 106653. https://doi.org/10.1016/j.ecolind.2020.106653

Selvakumar, S., Chandrasekar, N., & Kumar, G. (2017). Hydrogeochemical Characteristics and Groundwater Contamination in the Rapid Urban Development Areas of Coimbatore, India. *Water Resources and Industry, 17,* 26-33. https://doi.org/10.1016/j.wri.2017.02.002

Sheikhi, S., Faraji, Z., & Aslani, H. (2021). Arsenic Health Risk Assessment and the Evaluation of Groundwater Quality Using GWQI and Multivariate Statistical Analysis in Rural Areas, Hashtroud, Iran. *Environmental Science and Pollution Research, 28,* 3617-3631. https://doi.org/10.1007/s11356-020-10710-6

Shuaibu, A., Kalin, R. M., Phoenix, V., & Lawal, I. M. (2025). Geochemical Evolution and Mechanisms Controlling Groundwater Chemistry in the Transboundary Komadugu-Yobe Basin, Lake Chad Region: An Inte-grated Approach of Chemometric Analysis and Geochemical Modeling. *Journal of Hydrology: Regional Studies, 57,* Article ID: 102098.

Singhal, A., Gupta, R., Singh, A. N., & Shrinivas, A. (2020). Assessment and Monitoring of Groundwater Quality in Semi-Arid Region. *Groundwater for Sustainable Development, 11,* Article ID: 100381. https://doi.org/10.1016/j.gsd.2020.100381

Sivakarun, N., Udayaganesan, P., Chidambaram, S., Venkatramanan, S., Prasanna, M. V., Pradeep, K. et al. (2020). Factors Determining the Hydrogeochemical Processes Occurring in Shallow Groundwater of Coastal Alluvial Aquifer, India. *Geochemistry, 80,* Article ID: 125623. https://doi.org/10.1016/j.chemer.2020.125623

Subba Rao, N. (2017). Controlling Factors of Fluoride in Groundwater in a Part of South India. *Arabian Journal of Geosciences, 10,* Article No. 524. https://doi.org/10.1007/s12517-017-3291-7

Subba Rao, N. S., Dinakar, A., & Kumari, B. K. (2021). Appraisal of Vulnerable Zones of Non-Cancer-Causing Health Risks Associated with Exposure of Nitrate and Fluoride in Groundwater from a Rural Part of India. *Environmental Research, 202,* Article ID: 111674. https://doi.org/10.1016/j.envres.2021.111674

Tine, A. K., Issa, M., Sophie, A., Essouli, O. F., & Sarr, B. (2011). Réactualisation de la situation hydrogéologique des aquifères du maastrichtien et du paléocène de la région de Mbour, Sénégal. *Journal des Sciences et Technologies, 9,* 23-32.

Tokazhanov, G., Ramazanova, E., Hamid, S., Bae, S., & Lee, W. (2020). Advances in the Catalytic Reduction of Nitrate by Metallic Catalysts for High Efficiency and N2 Selectivity: A Review. *Chemical Engineering Journal, 384,* Article ID: 123252. https://doi.org/10.1016/j.cej.2019.123252

Tongesayi, S., & Tongesayi, T. (2017). Water Quality and Public Health. In S. Ahuja (Ed.), *Chemistry and Water* (pp. 553-596). Elsevier. https://doi.org/10.1016/b978-0-12-809330-6.00017-9

Torres-Martínez, J. A., Mora, A., Mahlknecht, J., Daesslé, L. W., Cervantes-Avilés, P. A., &

Ledesma-Ruiz, R. (2021). Estimation of Nitrate Pollution Sources and Transformations in Groundwater of an Intensive Livestock-Agricultural Area (Comarca Lagunera), Combining Major Ions, Stable Isotopes and Mixsiar Model. *Environmental Pollution, 269,* Article ID: 115445. https://doi.org/10.1016/j.envpol.2020.115445

Travi, Y. (1993). *Hydrogéologie et hydrochimie des aquifères du Sénégal. Hydrogéochimie du fluor dans les eaux souterraines*. Institut de Géologie-Université Louis-Pasteur, 3-158.

Travi, Y., & Le Coustour, E. (1982). Fluorose dentaire et eaux souterraines: L'exemple du Sénégal. *Eau du Québec, 15,* 9-12.

Tutmez, B., Hatipoglu, Z., & Kaymak, U. (2006). Modelling Electrical Conductivity of Groundwater Using an Adaptive Neuro-Fuzzy Inference System. *Computers & Geosciences, 32,* 421-433. https://doi.org/10.1016/j.cageo.2005.07.003

Wang, W., Li, W., Xue, M., Gu, X., Ye, C., Jiao, Y. et al. (2023). Spatial-Temporal Characteristics and Influencing Factors of Lake Water and Groundwater Chemistry in Hulun Lake, Northeast China. *Water, 15,* Article 937. https://doi.org/10.3390/w15050937

World Health Organization (WHO) (2017). *Guidelines for Drinking-Water Quality: Fourth Edition Incorporating the First Addendum.* https://iris.who.int/server/api/core/bitstreams/1b7a285e-3635-45dd-a1a9-6068c8fbe173/content

World Health Organization (WHO) (2022). *Guidelines for Drinking-Water Quality (Fourth Edition Incorporating the First and Second Addenda).* World Health Organization.

Xiao, J., Jin, Z., & Wang, J. (2014). Assessment of the Hydrogeochemistry and Groundwater Quality of the Tarim River Basin in an Extreme Arid Region, NW China. *Environmental Management, 53,* 135-146. https://doi.org/10.1007/s00267-013-0198-2

Xu, Y., & Shao, W. (2010). Groundwater Quality Evaluation in Yang Village by Fuzzy Mathematics Method. In *2010 International Conference on Digital Manufacturing & Automation* (pp. 790-794). IEEE. https://doi.org/10.1109/icdma.2010.445

Yang, J., Ye, M., Tang, Z., Jiao, T., Song, X., Pei, Y. et al. (2020). Using Cluster Analysis for Understanding Spatial and Temporal Patterns and Controlling Factors of Groundwater Geochemistry in a Regional Aquifer. *Journal of Hydrology, 583,* Article ID: 124594. https://doi.org/10.1016/j.jhydrol.2020.124594

Yu, N., Lv, Y., Liu, G., Zhuang, F., & Wang, Q. (2023). Spatial-Temporal Changes in Shallow Groundwater Quality with Human Health Risk Assessment in the Luxi Plain (China). *Water, 15,* Article 4120. https://doi.org/10.3390/w15234120

Zaidi, F. K., Nazzal, Y., Jafri, M. K., Naeem, M., & Ahmed, I. (2015). Reverse Ion Exchange as a Major Process Controlling the Groundwater Chemistry in an Arid Environment: A Case Study from Northwestern Saudi Arabia. *Environmental Monitoring and Assessment, 187,* Article No. 607. https://doi.org/10.1007/s10661-015-4828-4

Zhang, B., Zhao, D., Zhou, P., Qu, S., Liao, F., & Wang, G. (2020). Hydrochemical Characteristics of Groundwater and Dominant Water-Rock Interactions in the Delingha Area, Qaidam Basin, Northwest China. *Water, 12,* Article 836. https://doi.org/10.3390/w12030836

Zhang, Q., Qian, H., Xu, P., Hou, K., & Yang, F. (2021). Groundwater Quality Assessment Using a New Integrated-Weight Water Quality Index (IWQI) and Driver Analysis in the Jiaokou Irrigation District, China. *Ecotoxicology and Environmental Safety, 212,* Article ID: 111992. https://doi.org/10.1016/j.ecoenv.2021.111992

Zhang, T., Cai, W., Li, Y., Geng, T., Zhang, Z., Lv, Y. et al. (2018). Ion Chemistry of Groundwater and the Possible Controls within Lhasa River Basin, SW Tibetan Plateau. *Arabian Journal of Geosciences, 11,* Article No. 510. https://doi.org/10.1007/s12517-018-3855-1